Available online at www.CivileJournal.org

Civil Engineering Journal

Vol. 4, No. 5, May, 2018

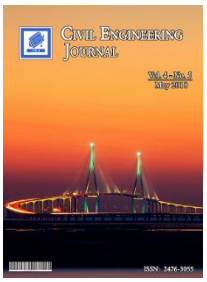

Evaluation of the P-Delta Effect on Collapse Capacity of Adjacent Structures Subjected to Far-field Ground Motions

Farzin Kazemi [a], Benyamin Mohebi [b*], Mansoor Yakhchalian [b]

[a] MSc in Earthquake Engineering, Faculty of Engineering and Technology, Imam Khomeini International University, Qazvin, Iran.

[b] Assistant Professor, Faculty of Engineering and Technology, Imam Khomeini International University, Qazvin, Iran.

Received 27 January 2018; Accepted 12 May 2018

Abstract

In urban areas, adjacent structures can be seen in any insufficient distance from each other, because of economic reasons and refusal of acquired minimum separation distance according to seismic previsions. Collapse capacity assessment of structures is one of the important objectives of performance-based seismic engineering. The purpose of this study is to consider the pounding phenomenon and P-Delta effect in seismic collapse capacity assessment of structures. For this purpose, 2-, 4-, 6- and 8-story adjacent structures with different conditions of separation distance among them, were modeled in the OpenSees software. Furthermore, Incremental Dynamic Analyses (IDAs) were performed using 78 far-field ground motion records to compute the collapse capacities of adjacent structures. The results obtained from IDAs for adjacent structures show that during pounding, taller structure reaches its collapse capacity earlier than shorter one. In addition, by considering the P-Delta effect and increasing the distance between adjacent structures, time of collapse and number of impacts increases. According to results, considering the P-Delta effect in modeling has significant influence in seismic collapse capacity assessment of pounding structures.

Keywords: P-Delta Effect; Collapse Capacity; Pounding Phenomenon; Linear Viscoelastic Element; Incremental Dynamic Analysis.

1. Introduction

Recent studies show that impact forces generated between two pounding structures have significant influence on dynamic behavior of both the structures and may cause higher story shear forces. When adjacent structures have different dynamic characteristics, if they do not have a sufficient separation distance from each other, they may collide resulting in critical impact forces especially on roof levels. To prevent the occurrence of the pounding phenomenon during an earthquake, seismic provisions prescribe providing a minimum seismic separation distance between adjacent structures. However, for a large number of existing buildings not designed according to seismic provisions this separation distance has not been considered, and therefore structural pounding during earthquakes is expected.

Collapse is a state that structure or a part of it loses its ability to withstand gravity loads under strong ground motions, and the P-Delta effect exacerbates this instability. Owing to the fact that the P-Delta effect can influence the stability of structure, many studies have investigated considering the P-Delta effect in modeling [1-4]. The P-Delta effect induces additional moments because of lateral deformations and axial gravity loads. The magnitude of P-Delta effect is related to the lateral deformation, Delta, and axial load, P [5, 6]. Adam and Jäger [7] introduced a collapse assessment methodology to assess the P-Delta effect on the seismic collapse capacity of Single-Degree-of-Freedom (SDOF) systems by means of the so-called collapse capacity spectra. They used 44 far-field ground motion records for creating collapse capacity spectra to assess the dynamic stability of multi-story structures. Black [8] derived two closed-form expressions

* Corresponding author: mohebi@eng.ikiu.ac.ir

http://dx.doi.org/10.28991/cej-0309156

from analytical considerations for quantifying the P-Delta effect in moment-resisting frames. He used two stability coefficients, which are called the modal-elastic and the modal-inelastic, to precisely predict base shear-deformation curve by considering the P-Delta effect. Considering appropriate seismic intensity measure (IM) is important for nonlinear dynamic analyses. Tsantaki et al. [9] proposed two IMs to reduce the collapse capacity dispersion of SDOF systems that are vulnerable to the P-Delta effect. The collapse capacity dispersion is caused by the ground motion variability and the variations of frequency content of ground motions. Adam et al. [10] proposed an optimal IM for assessing the seismic collapse capacity of generic moment frames vulnerable to the P-Delta effect. This IM, which is derived from the geometric mean of pseudo-spectral accelerations over a range of periods, provides minimum dispersion for the entire set of purely P-Delta vulnerable frames with different number of stories and fundamental periods of vibration. Yakhchalian et al. [11, 12] proposed new proxies for ground motion record selection for seismic collapse assessment of short-period and long-period structures. Using these proxies causes reduction in collapse capacity dispersion. Belleri et al. [13] considered the Displacement-Based Assessment (DBA) procedure for evaluating the P-Delta effect on SDOF like structures. They showed that the P-Delta effect reduces the lateral load associated to a displacement, afterward leading to a decrease in effective stiffness and an increase in the effective period. Ucar and Merter [14] proposed a modified energy-balance equation for the P-Delta effect by adding the external work of gravity loads. They concluded that by increasing the number of stories, with and without considering the P-Delta effect, energy-based base shear force decreases. Therefore, their derived an equation that provides a good estimation of the base shear force of Multi-Degree-of-Freedom (MDOF) structures. Adam and Jäger [15] proposed a simplified collapse assessment methodology based on pushover analyses for regular moment-resisting frame structures. For modeling 15-, 18-, 21- and 24-story structures, they used moment-resisting single-bay frames that had fundamental periods of vibration equal to 0.2N, where N is the number of stories. By using this type of modeling, it was possible to investigate the collapse capacity of structures, which requires computationally expensive Incremental Dynamic Analyses (IDAs). Gharyanpoor et al. [16] evaluated the seismic collapse capacity of SDOF systems equipped with fluid viscous dampers considering the P-Delta effect. They concluded that the P-delta effect controls the collapse capacity of long-period SDOF systems.

Madani et al. [17] considered different cases of 3- to 12-story adjacent structures for evaluating the effects of structural pounding and Structure-Soil-Structure Interaction (SSSI). Although they conducted a comprehensive study on the pounding phenomenon and SSSI effect, they did not consider the P-Delta effect in modeling. According to their study, seismic damage in columns increases by increasing the distance of adjacent structures. In addition, considering the SSSI effect causes the pounding phenomenon even at farther distances, and pounding between structures causes increase in story shear forces and lateral displacements especially in taller structure.

Although the P-Delta effect has been focused in many studies excluding the pounding phenomenon, but impact forces because of pounding of adjacent structures can change the structural response and cause the P-Delta effect more crucial. In other words, pounding of adjacent structures increases the lateral deformations of stories especially in first story, so these added deformations can increase the P-Delta effect. This study investigates the seismic collapse capacity of the adjacent pounding structures, with and without considering the P-Delta effect. For this purpose, 2-, 4-, 6- and 8-story nonlinear MDOF stick models assuming different values of separation distance among them are considered, and a linear viscoelastic contact element is used for simulating the pounding phenomenon between the adjacent structures. The results indicate that considering the P-Delta effect has a great influence on seismic collapse capacity predictions.

2. Modeling Approaches

In this study, 2-, 4- and 6-story moderately ductile, and 6- and 8-story highly ductile structures were considered. In this section, the modeling approaches used to simulate pounding phenomenon and the nonlinear behavior of the structures considered are described. OpenSees [18] software was used for the simulation of pounding structures. Jankowski and Mahmoud [19] compared the results of numerical analyses with the results of experiments conducted by dropping concrete, steel and timber ball onto a rigid surface with the same material. Then, the impact force time histories during the experiments were compared with the results of numerical analyses achieved using linear elastic, linear viscoelastic, modified linear viscoelastic, Hertz non-linear elastic, Hertzdamp non-linear and non-linear viscoelastic contact element models. The results of their study showed that the linear viscoelastic contact element model had a normalized root mean square (RMS) error of 11.7%, which is less than others contact element models. According to these results and considering concrete-to-concrete impact, the linear viscoelastic model (Kelvin-Voigt model), which consists of a linear spring and a viscous damper, was used in this study for simulating the pounding phenomenon. Figure 1 shows a typical linear viscoelastic model between two SDOF systems. The linear viscoelastic contact element model can consider the energy dissipation in pounding phenomenon.

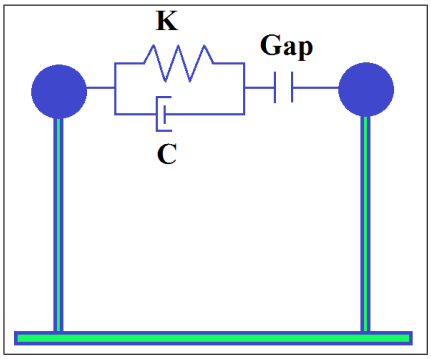

Figure 1. A typical linear viscoelastic model between two SDOF systems

The pounding force when using this contact element model, is expressed as:

$$F(t)=K\delta(t)+C\dot{\delta}(t) \quad (1)$$

Where $\delta(t)$ describes the relative deformation between pounding structural members, and $\dot{\delta}(t)$ denotes the relative velocity between them, K is the impact element's stiffness and C is the impact element's damping [20, 21].

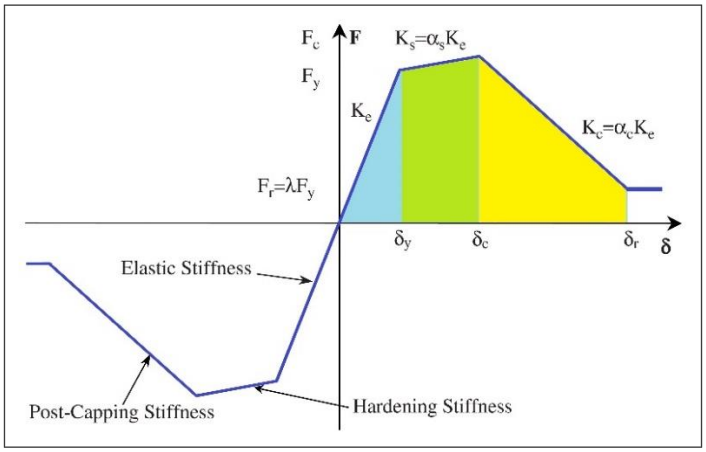

Figure 2. Backbone curve of all stories

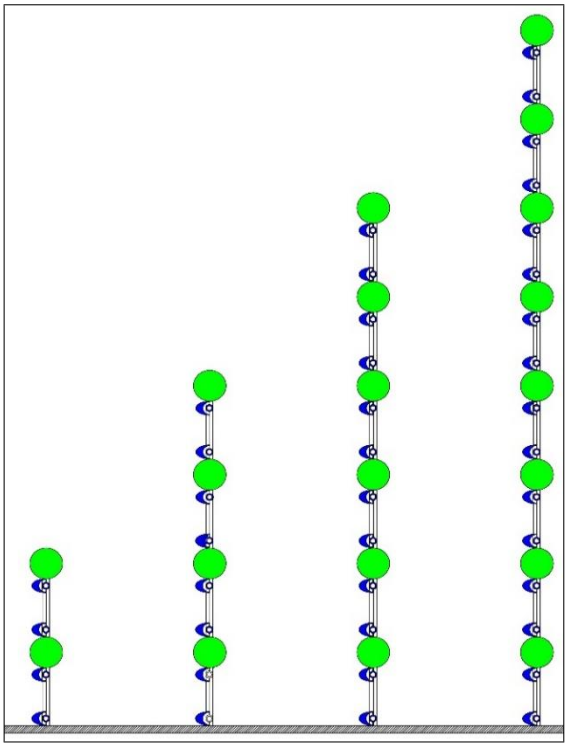

Figure 3. Stick models of the 2-, 4-, 6- and 8-story structures

To model the nonlinear behavior of the stick models, which consist of elastic beam-column elements and nonlinear zero-length elements, bilinear Ibarra-Medina-Krawinkler model [22] was applied. Figure 2 indicates the backbone curve of each story, where K_e is the elastic stiffness of story, $K_s = \alpha_s K_e$ is the hardening stiffness of story, and $K_c = \alpha_c K_e$ is the post-capping stiffness of story. In this study, the hardening coefficient, αs, and post-capping coefficient, αc, used to simulate the nonlinear behaviour of all stories were assumed as 0.03 and -0.1, respectively. In addition, for moderately ductile and highly ductile structures, representing intermediate and special moment-resisting frames, $\mu = \delta_c/\delta_y$ was assumed equal to 4.0 and 6.0, respectively. Figure 3 indicates the stick models of the 2-, 4-, 6- and 8-story structures. To model these structures, their fundamental periods, T1, were assumed equal to 0.2 N, where N is the number of stories, and the height of stories were considered equal to 3.6 m. The yield base shears of all the structures were determined using ASCE 7-10 [23] and nonlinear static analysis. By applying the linear viscoelastic model to simulate the impact phenomenon, four values of separation distance equal to 0.0, 0.5D, 1.0D and 1.5D were considered, where D is equal to the separation distance prescribed by ASCE 7-10 [23].

3. Collapse Capacity Assessment of the Structures

To capture the effect of record-to-record variability, IDAs were performed using 78 far-field ground motion records used by Haselton [24]. The selected records for IDAs are listed in Table 1. Sa (T1) was selected as IM for performing IDAs and the Hunt and Fill algorithm was applied [25]. Figures 4 and 5 illustrate the IDA curves for the 2-story and 8-story pounding structures, without considering the P-Delta effect, and the 2-story and 6-story pounding structures, with considering the P-Delta effect, given the separation distance equal to 1.0D, respectively. Each black line in this figure represents an IDA curve corresponding to a record and the bold red line represents the median of the IDA curves. The flattening of each curve represents the point corresponding to the collapse capacity of the structure. For instance, the median collapse capacities of the 2-story and 8-story pounding structures without considering the P-Delta effect are equal to 3.48 and 0.42 g respectively.

Table 1. Characteristics of the far-field ground motion records used by Haselton [24]

EQ Index	EQ ID	PEERNGA Rec. Num.	Mag.	Year	Event	Fault Type	Campbell Distance (km)	Joyner-Boore Distance (km)
1	12011	953	6.7	1994	Northridge	Blind thrust	17.2	9.4
2	12012	960	6.7	1994	Northridge	Blind thrust	12.4	11.4
3	12013	1003	6.7	1994	Northridge	Blind thrust	27	21.2
4	12014	1077	6.7	1994	Northridge	Blind thrust	27	17.3
5	12015	952	6.7	1994	Northridge	Blind thrust	18.4	12.4
6	12041	1602	7.1	1999	Duzce,Turkey	Strike-slip	12.4	12
7	12052	1787	7.1	1999	Hector Mine	Strike-slip	12	10.4
8	12061	169	6.5	1979	Imperial Valley	Strike-slip	22.5	22
9	12062	174	6.5	1979	Imperial Valley	Strike-slip	13.5	12.5
10	12063	162	6.5	1979	Imperial Valley	Strike-slip	11.6	10.5
11	12064	189	6.5	1979	Imperial Valley	Strike-slip	10.8	9.6
12	12071	1111	6.9	1995	Kobe, Japan	Strike-slip	25.2	7.1
13	12072	1116	6.9	1995	Kobe, Japan	Strike-slip	28.5	19.1
14	12073	1107	6.9	1995	Kobe, Japan	Strike-slip	3.2	22.5
15	12074	1106	7.5	1995	Kobe, Japan	Strike-slip	95.8	0.9
16	12081	1158	7.5	1999	Kocaeli,Turkey	Strike-slip	15.4	13.6
17	12082	1148	7.3	1999	Kocaeli,Turkey	Strike-slip	13.5	10.6
18	12091	900	7.3	1992	Landers	Strike-slip	23.8	23.6
19	12092	848	7.3	1992	Landers	Strike-slip	20	19.7
20	12093	864	7.3	1992	Landers	Strike-slip	11.4	11
21	12101	752	6.9	1989	Loma Prieta	Strike-slip	35.5	8.7
22	12102	767	6.9	1989	Loma Prieta	Strike-slip	12.8	12.2
23	12103	783	6.9	1989	Loma Prieta	Strike-slip	74.3	74.2
24	12104	776	6.9	1989	Loma Prieta	Strike-slip	27.9	27.7
25	12105	777	6.9	1989	Loma Prieta	Strike-slip	27.6	27.4
26	12106	778	6.9	1989	Loma Prieta	Strike-slip	24.8	24.5
27	12111	1633	7.4	1990	Manjil, Iran	Strike-slip	13	12.6

28	12121	721	6.5	1987	Superstition Hills	Strike-slip	18.5	18.2
29	12122	725	6.5	1987	Superstition Hills	Strike-slip	11.7	11.2
30	12123	728	6.5	1987	Superstition Hills	Strike-slip	13.5	13
31	12132	829	7	1992	Cape Mendocino	Thrust	14.3	7.9
32	12141	1244	7.6	1999	Chi-Chi,Taiwan	Thrust	15.5	10
33	12142	1485	7.6	1999	Chi-Chi,Taiwan	Thrust	26.8	26
34	12143	1524	7.6	1999	Chi-Chi,Taiwan	Thrust	45.3	45.2
35	12144	1506	7.6	1999	Chi-Chi,Taiwan	Thrust	24.4	19
36	12145	1595	7.6	1999	Chi-Chi,Taiwan	Thrust	15.4	10
37	12146	1182	7.6	1999	Chi-Chi,Taiwan	Thrust	13.2	9.8
38	12151	68	6.6	1971	San Fernando	Thrust	25.8	22.8
39	12171	125	6.5	1976	Friuli, Italy	Thrust	15.8	15

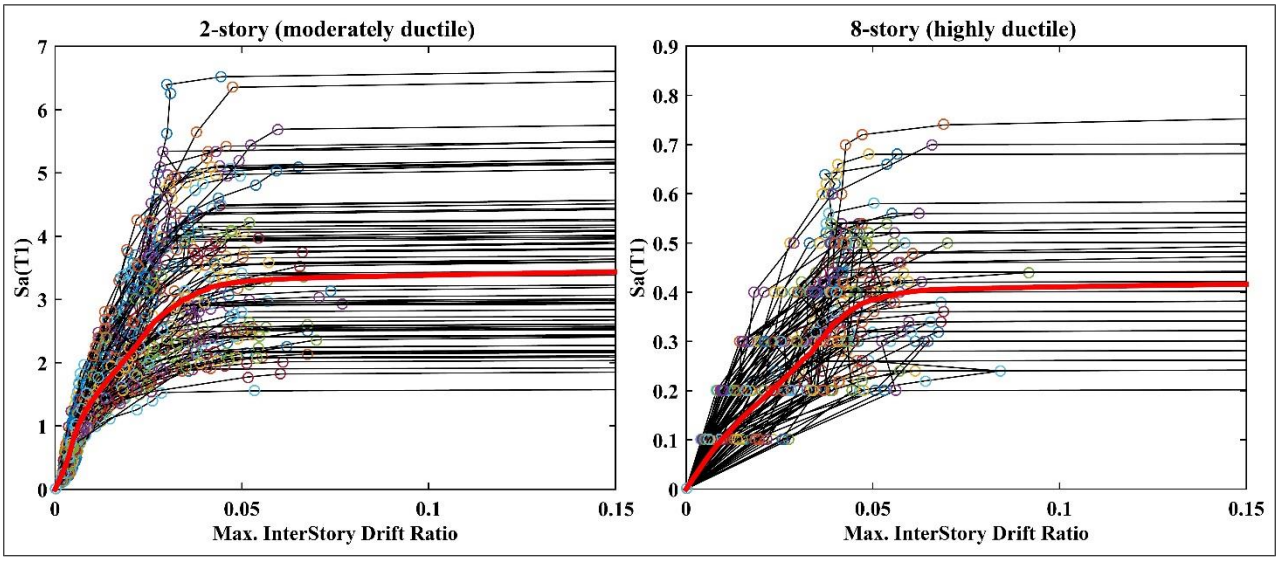

Figure 4. IDA curves for the 2-story and 8-story pounding structures without considering the P-Delta effect at separation distance equal to 1.0D

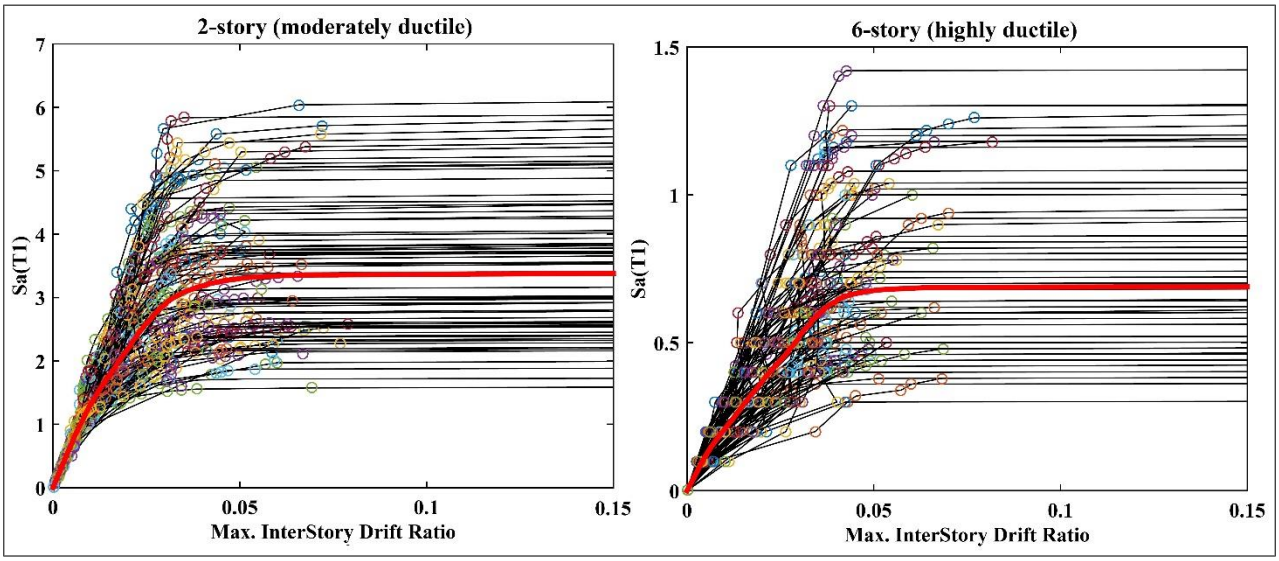

Figure 5. IDA curves for the 2-story and 6-story pounding structures with considering the P-Delta effect at separation distance equal to 1.0D

4. P-Delta Effect on Collapse Capacity of the Structures

To investigate the impact force due to pounding phenomenon, the impact force in each floor was calculated through

the linear viscoelastic contact element model. Figures 6 to 8 present the impact force time-histories for the 4-story and 8-story pounding structures subjected to a record of the Northridge earthquake (Beverly Hills, USC station 90014), given Sa(T1) =2.6g, with considering the P-Delta effect and the three aforementioned separation distances, equal to 0.0D, 0.5D and 1.0D, respectively.

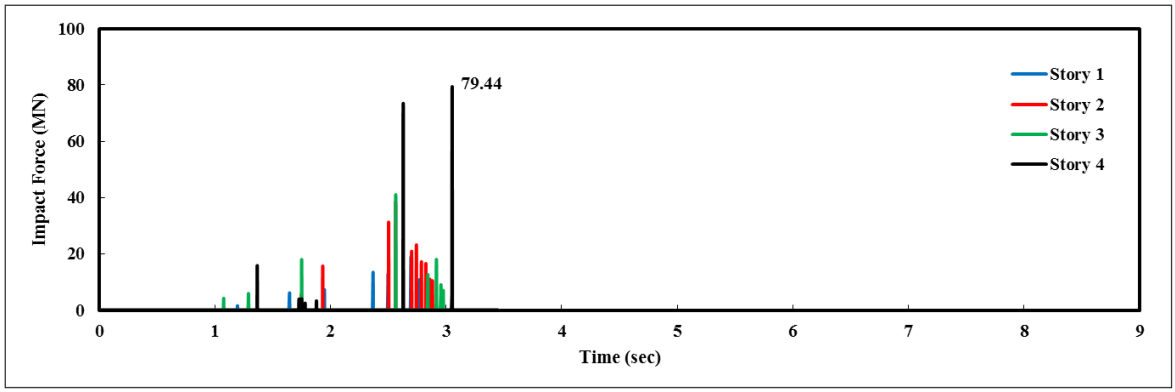

Figure 6. Impact force time-histories corresponding to the stories 1 to 4 of the 4-story and 8-story pounding structures with considering the P-Delta effect and the separation distance equal to 0.0D

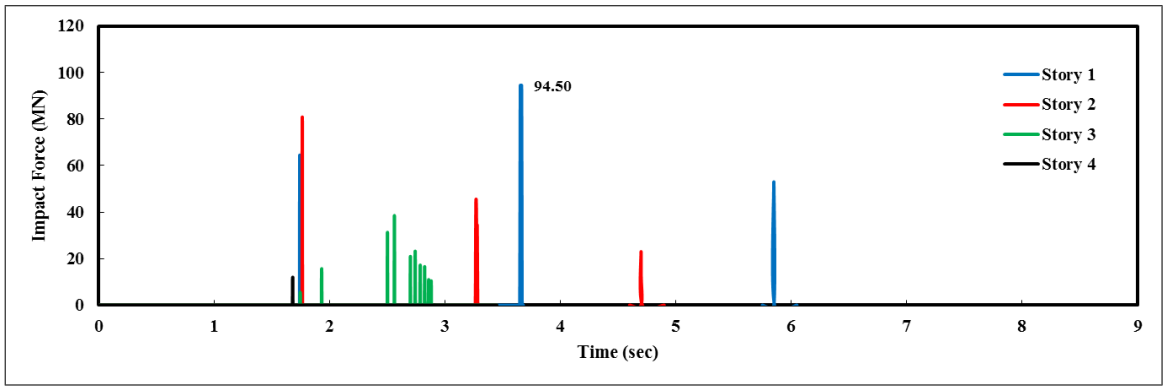

Figure 7. Impact force time-histories corresponding to the stories 1 to 4 of the 4-story and 8-story pounding structures with considering the P-Delta effect and the separation distance equal to 0.5D

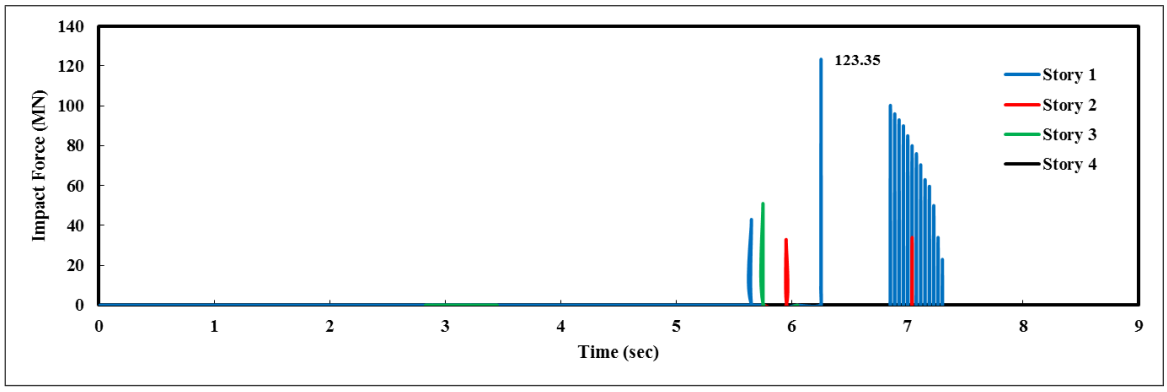

Figure 8. Impact force time-histories corresponding to the stories 1 to 4 of the 4-story and 8-story pounding structures with considering the P-Delta effect and the separation distance equal to 1.0D

Figure 6 indicates that given the separation distance equal to 0.0, the maximum impact force occurs in the 4th story. According to Figure 7 and 8, increasing the separation distance to 0.5D and 1.0D leads to the maximum impact force occurring in the first story. The results obtained in these figures indicate that as the separation distance between adjacent structures increases from 0.0 to 1.0D, the maximum impact force increases from 79.44 to 123.35 MN. Furthermore, increasing the separation distance from 0.0 to 1.0D, increases the collapse time from 4.17 to 8.34 sec. Therefore, the collapse time and number of impacts in the first floor increases with increasing the separation distance between two pounding structures. Figure 9 presents the impact force time-histories of the 4-story and 8-story structures without considering the P-Delta effect. Comparing Figures 8 and 9 indicates that considering the P-Delta effect influences the impact force values significantly. Although the results of impact forces for the 4-story and 8-story pounding structures

are presented for the Northridge earthquake, similar results were obtained from the other considered pounding structures and ground motion records.

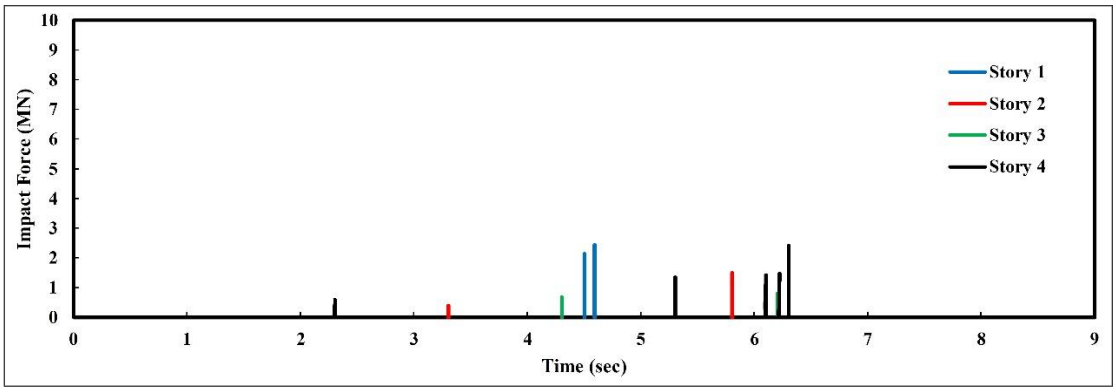

Figure 9. Impact force time-histories corresponding to the stories 1 to 4 of the 4-story and 8-story pounding structures without considering the P-Delta effect and the separation distance equal to 1.0D

To investigate the results of IDAs, the median collapse capacity of each of two pounding structures with and without considering the P-Delta effect are compared. Figure 10 presents the median collapse capacity of the 2-story and 8-story pounding structures given the four aforementioned separation distances. According to this figure, taking the P-Delta effect into account the median collapse capacity of the 2-story and 8-story structures decreases by an average of 6% and 45%, respectively. Therefore, it is obvious that taking the P-Delta effect into account has more influence on the median collapse capacity of the taller structure. Although in this section only the IDA results of the 2-story and 8-story pounding structures are presented, the same results for the other pounding structures were observed.

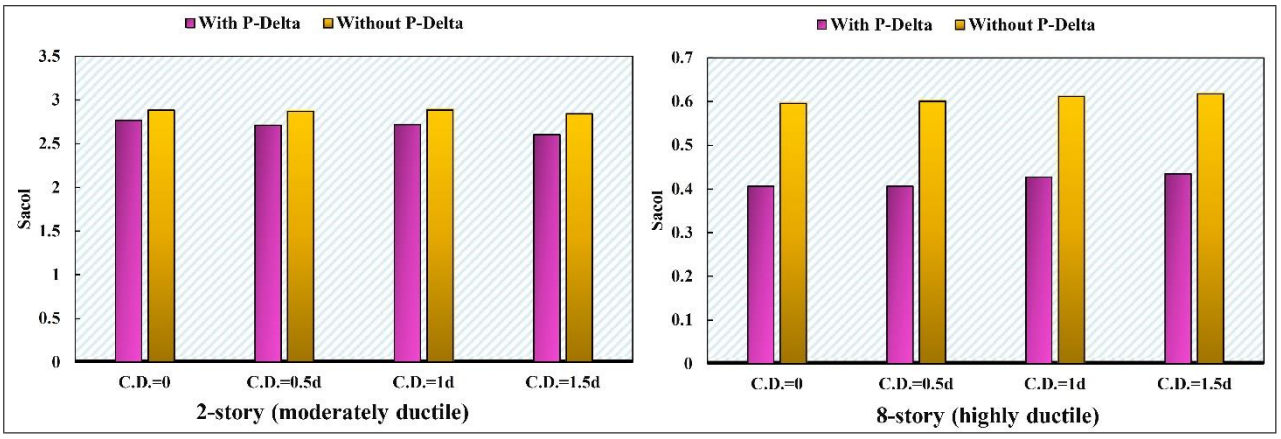

Figure 10. The P-Delta effect on the median collapse capacity of the 2-story and 8-story pounding structures

5. Conclusion

In this study, 2-, 4-, 6- and 8-story nonlinear MDOF stick models assuming four values of separation distance among them were considered to evaluate the seismic collapse capacity of pounding structures, with and without accounting for the P-Delta effect. A linear viscoelastic contact element model was used to simulate the impact phenomenon between pounding structures modeled using OpenSees software. Moreover, to obtain the seismic collapse capacity of pounding structures, Incremental Dynamic Analyses (IDAs) were performed using 78 far-field ground motion records. The results show that as the separation distance between two adjacent pounding structures increases, the maximum impact force especially in lower stories, the collapse time and the number of impacts in the first floor increase correspondingly. Moreover, considering the P-Delta effect increases the impact forces significantly. Based on the results, it can be seen that considering the P-Delta effect causes decrease in the median collapse capacity of each of the pounding structures. In the case of pounding between a shorter structure and a taller one, the P-Delta effect has more influence on the median collapse capacity of the taller structure. Therefore, in the pounding of two adjacent structures with different heights, the P-Delta effect is the main factor causing the collapse of the taller structure.

6. References

[1] Jennings, Paul C., and Raul Husid. "Collapse of yielding structures during earthquakes." Journal of Engineering Mechanics (1968): doi: 10.1016/b978-0-12-812975-3.15004-2.

[2] Bernal, Dionisio. "Instability of buildings subjected to earthquakes." Journal of Structural Engineering 118.8 (1992): 2239-2260:

doi: 10.1061/0733-9445(1992)118:8(2239).

[3] MacRae, Gregory A. "P-Δ effects on single-degree-of-freedom structures in earthquakes." Earthquake Spectra 10.3 (1994): 539-568: doi: 10.1193/1.1585788.

[4] Bernal, Dionisio. "Instability of buildings during seismic response." Engineering Structures 20.4-6 (1998): 496-502: doi: 10.1016/s0141-0296(97)00037-0.

[5] MacRae, Gregory A. "P-Δ effects on single-degree-of-freedom structures in earthquakes." Earthquake Spectra 10.3 (1994): 539-568: doi: 10.1193/1.1585788.

[6] Lignos, D. G., H. Krawinkler, and A. S. Whittaker. "Prediction and validation of sideway collapse of two scale models of a 4 - story steel moment frame." Earthquake Engineering & Structural Dynamics 40.7 (2011): 807-825: doi: 10.1002/eqe.1061.

[7] Adam, Christoph, and Clemens Jäger. "Seismic collapse capacity of basic inelastic structures vulnerable to the P - delta effect." Earthquake Engineering & Structural Dynamics 41.4 (2012): 775-793: doi: 10.1002/eqe.1157.

[8] Black, E. F. "Use of stability coefficients for evaluating the P–Δ effect in regular steel moment resisting frames." Engineering Structures 33.4 (2011): doi: 1205-1216. 10.1016/j.engstruct.2011.09.011.

[9] Tsantaki, Styliani, Christoph Adam, and Luis F. Ibarra. "Intensity measures that reduce collapse capacity dispersion of P-delta vulnerable simple systems." Bulletin of Earthquake Engineering 15.3 (2017): doi: 1085-1109. 10.1007/s10518-016-9994-4.

[10] Adam, Christoph, et al. "Optimal Spectral Acceleration-based Intensity Measure for Seismic Collapse Assessment of P-Delta Vulnerable Frame Structures." Journal of Earthquake Engineering 21.7 (2017): doi: 1189-1195. 10.1080 /13632469.2016.1210059.

[11] Yakhchalian, M., Gholamreza Ghodrati Amiri, and Mahdi Eghbali. "Reliable Seismic Collapse Assessment of Short-Period Structures Using New Proxies for Ground Motion Record Selection." Scientia Iranica 0, no. 0 (August 13, 2017): 0–0. doi:10.24200/sci.2017.4162.

[12] Yakhchalian, Masood, Gholamreza Ghodrati Amiri, and Ahmad Nicknam. "A New Proxy for Ground Motion Selection in Seismic Collapse Assessment of Tall Buildings." The Structural Design of Tall and Special Buildings 23, no. 17 (November 20, 2013): 1275–1293. doi:10.1002/tal.1143.

[13] Belleri, Andrea, et al. "A Novel Framework to Include P-Δ Effects in Displacement-Based Seismic Assessment." Journal of Earthquake Engineering 21.3 (2017): doi: 486-492. 10.1080/13632469.2016.1178193.

[14] Ucar, Taner, and Onur Merter. "Derivation of energy-based base shear force coefficient considering hysteretic behavior and P-delta effects." Earthquake Engineering and Engineering Vibration 17.1 (2018): doi: 149-163. 10.1007 /s11803-018-0431-3.

[15] Adam, Christoph, and Clemens Jäger. "Simplified collapse capacity assessment of earthquake excited regular frame structures vulnerable to P-delta." Engineering Structures 44 (2012): doi: 159-173. 10.1016/j.engstruct.2012.05. 036.

[16] Gharyanpoor, Zeynab, Benyamin Mohebi, and Mansoor Yakhchalian. "COLLAPSE CAPACITY PREDICTION OF SDOF SYSTEMS EQUIPPED WITH FLUID VISCOUS DAMPERS." Proceedings of the 6th International Conference on Computational Methods in Structural Dynamics and Earthquake Engineering (COMPDYN 2017) doi:10.7712/120117.5705.18225.

[17] Madani, B., F. Behnamfar, and H. Tajmir Riahi. "Dynamic response of structures subjected to pounding and structure–soil–structure interaction." Soil Dynamics and Earthquake Engineering 78 (2015): doi: 46-60. 10.1016 /j.soildyn.2015.07.002.

[18] McKenna, F., et al. "Open system for earthquake engineering simulation (OpenSees). Berkeley: Pacific Earthquake Engineering Research Center, University of California; 2005." (2016): doi: 1-17.10.1109/mcse.2011.66.

[19] Jankowski, Robert, and Sayed Mahmoud. Earthquake-induced structural pounding. Springer, 2016. doi: 10.1007/ 978-3-319-16324-6_2.

[20] Jankowski, Robert. "Non - linear viscoelastic modelling of earthquake - induced structural pounding." Earthquake engineering & structural dynamics 34.6 (2005): doi: 595-611. 10.1002/eqe.434.

[21] Rahman, A. M., A. J. Carr, and P. J. Moss. "Seismic pounding of a case of adjacent multiple-storey buildings of differing total heights considering soil flexibility effects." Bulletin of the New Zealand National Society for Earthquake Engineering 34.1 (2001): 40-59. doi: 10.12989/eas.2001.1.3.307.

[22] Altoontash, Arash. Simulation and damage models for performance assessment of reinforced concrete beam-column joints. Diss. Stanford University, 2004. doi: 10.5772/65490.

[23] American Society of Civil Engineers. Minimum design loads for buildings and other structures. Vol. 7. Amer Society of Civil Engineers, 2010. doi: 10.1061/9780784412916.err.

[24] Haselton, Curt B. "Assessing Seismic Collapse Safety of Modern Reinforced Concrete Moment Frame Buildings." Stanford University. (2006): doi: 10.1061/40944(249)22.

[25] Vamvatsikos, Dimitrios, and C. Allin Cornell. "Incremental dynamic analysis." Earthquake Engineering & Structural Dynamics 31.3 (2002): doi: 491-514. 10.1007/978-3-642-36197-5_136-1.